Elsevier Editorial System(tm) for Nuclear Inst. and Methods in Physics Research, A
Manuscript Draft

Manuscript Number: NIMA-D-18-00091R1

Title: Performance check of the CsI(Tl) calorimeter for the J-PARC E36 experiment by observing e^+ from muon decay

Article Type: Full length article

Section/Category: High Energy and Nuclear Physics Detectors

Keywords: Kaon decay; CsI(Tl) Calorimeter; Waveform Analysis

Corresponding Author: Dr. Hiroshi Ito,

Corresponding Author's Institution:

First Author: Hiroshi Ito

Order of Authors: Hiroshi Ito; Kate Horie, Ph D; Suguru Shimizu, Ph. D.; Sebastien Bianchin, Ph. D.; Chaden Djalali, Ph. D.; Bishoy Dongwi; David Gill, Ph. D.; Michael Hasinoff, Ph. D.; Yoichi Igarashi, Ph D; Jun Imazato, Ph. D.; N. Kalantarians, Ph. D.; Hideyuki Kawai, Ph. D.; Satoshi Kodama; Michael Kohl, Ph. D.; H. Lu, Ph D; O. Mineev; Makoto Tabata, Ph D; R. Tanuma; N. Yershov

Abstract: The J-PARC E36 experiment is searching for lepton universality violation with a stopped kaon beam by measuring the ratio of the K^+ decay widths $\Gamma(K_{e2})/\Gamma(K_{\mu2})=\Gamma(K^+\to e^+ \nu_e)/\Gamma(K^+\to \mu^+ \nu_\mu)$. Since the radiative ${K^+\to e^+ \nu_e \gamma}$ decays are backgrounds to be removed in this measurement, the radiated γ rays were detected in a CsI(Tl) calorimeter. The energy calibration for the 768 CsI(Tl) modules was performed using mono-chromatic μ^+s from the $K_{\mu2}$ decays. The delayed e^+ signals from the muon decays were required in order to improve the S/N ratio of the $K_{\mu2}$ peak by suppressing background events. In addition, a new energy calibration method of the CsI(Tl) calorimeter using stopped cosmic muons has been established.

Performance check of the CsI(Tl) calorimeter for the J-PARC E36 experiment by observing e^+ from muon decay

H. Ito[a,*], K. Horie[b], S. Shimizu[b,**], S. Bianchin[c], C. Djalali[d], B. Dongwi[e], D. Gill[c], M. Hasinoff[f], Y. Igarashi[g], J. Imazato[g], N. Kalantarians[h], H. Kawai[i], S. Kimura[i], A. Kobayashi[i], S. Kodama[i], M. Kohl[e], H. Lu[d], O. Mineev[j], M. Tabata[i], R. Tanuma[k], N. Yershov[j]

[a] *Department of Physics, Kobe University, Hyogo, 657-8501, Japan*
[b] *Department of Physics, Osaka University, Osaka, 560-0043, Japan*
[c] *TRIUMF, Vancouver, V6T 2A3, Canada*
[d] *Department of Physics and Astronomy, University of Iowa, Iowa City, IA 52242, USA*
[e] *Physics Department, Hampton University, VA 23668, USA*
[f] *Department of Physics and Astronomy, University of British Columbia, Vancouver, V6T, 1Z1, Canada*
[g] *High Energy Accelerator Research Organization (KEK), Tsukuba, 305-0801, Japan*
[h] *Virginia Union University, Natural Science Department, Richmond VA, 23220, USA*
[i] *Department of Physics, Chiba University, Chiba, 263-8522, Japan*
[j] *Institute for Nuclear Research, Moscow, 117312, Russia*
[k] *Department of Physics, Rikkyo University, Toshima, 171-8501, Japan*

Abstract

The J-PARC E36 experiment is searching for lepton universality violation with a stopped kaon beam by measuring the ratio of the K^+ decay widths $\Gamma(K_{e2})/\Gamma(K_{\mu2}) = \Gamma(K^+ \to e^+\nu_e)/\Gamma(K^+ \to \mu^+\nu_\mu)$. Since the radiative $K^+ \to e^+\nu_e\gamma$ decays are backgrounds to be removed in this measurement, the radiated γ rays were detected in a CsI(Tl) calorimeter. The energy calibration for the 768 CsI(Tl) modules was performed using mono-chromatic μ^+s from the $K_{\mu2}$ decays. The delayed e^+ signals from the muon decays were required in order to improve the S/N ratio of the $K_{\mu2}$ peak by suppressing background events. In addition, a new energy calibration method of the CsI(Tl) calorimeter using stopped cosmic muons has been established.

Keywords: Kaon decay, CsI(Tl) calorimeter, Waveform analysis

1. Introduction

The $K^+ \to l^+\nu_l$ decay channel is one of the best processes to search for a lepton universality violation [1–3]. The ratio of $K^+ \to e^+\nu_e$ (K_{e2}) and $K^+ \to \mu^+\nu_\mu$ ($K_{\mu2}$) decay widths (R_K) can be very precisely calculated in the framework of the Standard Model (SM) under the assumption of μ–e universality as [4],

$$R_K^{\rm SM} = \frac{\Gamma(K_{e2})}{\Gamma(K_{\mu2})} = (2.477 \pm 0.001) \times 10^{-5}. \quad (1)$$

In order to compare the experimental R_K value with the SM prediction, the internal bremsstrahlung process in radiative $K^+ \to e^+\nu_e\gamma$ ($K_{e2\gamma}^{\rm IB}$) and $K^+ \to \mu^+\nu_\mu\gamma$ ($K_{\mu2\gamma}^{\rm IB}$) decay has to be included in the K_{e2} and $K_{\mu2}$ samples. On the other hand, the structure dependent processes in radiative $K^+ \to e^+\nu_e\gamma$ ($K_{e2\gamma}^{\rm SD}$) and $K^+ \to \mu^+\nu_\mu\gamma$ ($K_{\mu2\gamma}^{\rm SD}$) decays are backgrounds and should be removed in the analysis [3]. A deviation of the experimentally measured R_K from the SM value would lead to a μ–e universality violation and indicate the existence of New Physics beyond the SM.

The J-PARC E36 experiment aims to perform a precise R_K measurement by adopting a stopped K^+ beam method [5, 6]. The experiment was performed in 2015. A separated 800 MeV/c K^+ beam was slowed down by a degrader and stopped in a position sensitive K^+ stopper. The momentum measurement of the charged particles was performed using a 12-sector ion-core superconducting toroidal

*Corresponding author.
E-mail address: ito.hiroshi@crystal.kobe-u.ac.jp (H. Ito).
**Principal corresponding author.
E-mail address: suguru@phys.sci.osaka-u.ac.jp (S. Shimizu).

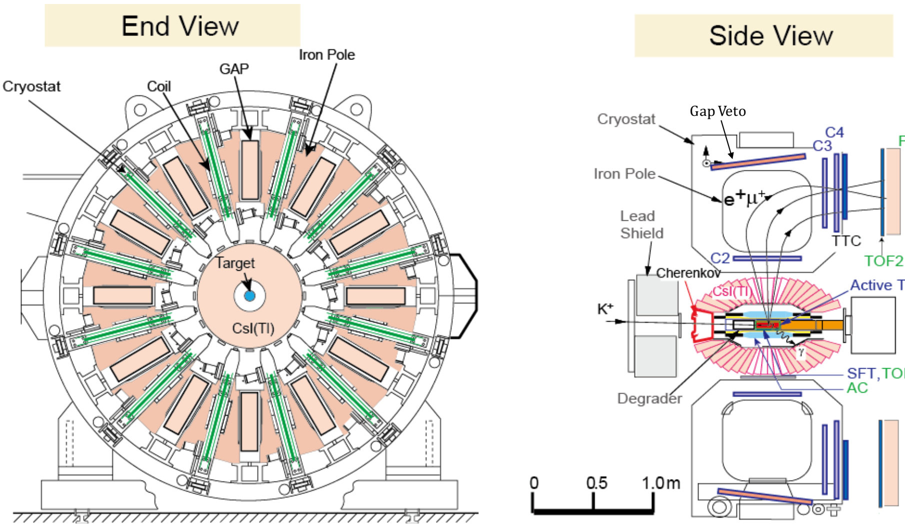

Fig. 1: Cross sectional end and side views of the setup for the J-PARC E36 experiment. The momentum vectors of charged particles and photons are determined by the toroidal spectrometer and the CsI(Tl) calorimeter, respectively.

spectrometer, as shown in Fig. 1. The radiated photon from the above radiative processes was measured by a CsI(Tl) calorimeter, an assembly of 768 CsI(Tl) crystals, which covers 75% of the total solid angle. The photon energy and hit position were obtained by summing the energy deposits and by determining the energy-weighted centroid, respectively. Since the SD component subtraction is one of the key issues in E36, the understanding of the CsI(Tl) performance is very important.

This paper is organized as follows. Details of the CsI(Tl) calorimeter and the analysis procedure are described in Section 2 and Section 3. In Section 4, a calibration method using the mono-chromatic μ^+s from the $K_{\mu 2}$ decays is explained. A new method of the CsI(Tl) energy calibration using stopped cosmic-ray muons is discussed in Section 5. The results obtained in the present studies are summarized in Section 6.

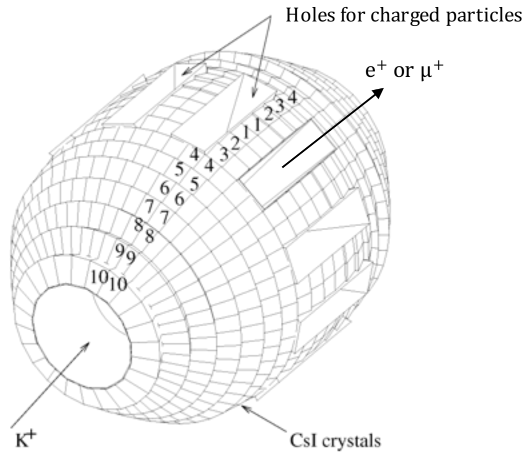

Fig. 2: The schematic view of the CsI(Tl) calorimeter. There were 12 holes for outgoing charged particles and 2 holes for the beam entrance and exit. Each crystal had a coverage of 7.5 ° along both the polar and azimuthal directions.

2. CsI(Tl) calorimeter

The CsI(Tl) calorimeter was originally constructed for the KEK-PS E246 experiment to search for a T-violating transverse muon polarization in $K^+ \to \pi^0 \mu^+ \nu_\mu$ decay [7–9]. There were 12 holes for outgoing charged particles and 2 holes for the beam entrance and exit, as shown in Fig. 2. Each crystal had a coverage of 7.5° along both the polar and azimuthal directions. The length of the CsI(Tl) crystal was 25 cm which was long enough to neglect shower leakage from the rear end.

Since the CsI(Tl) calorimeter had to be operated under a relatively strong fringing field from the toroidal magnet where PMTs would be difficult to use, PIN photodiodes (PIN diodes) were employed to read out the scintillation light of the CsI(Tl) crystals. Each crystal with its associated PIN diode and pre-amplifier was assembled in an Al container of 0.1 mm thickness. A charge sensitive pre-amplifier with a time constant of 600 μs and a gain of 0.5 V/pC was attached directly to the PIN diode. The output signal from the pre-amplifier was fed to a shaping amplifier with 1 μs shaping time. The waveforms of the shaping amplifier outputs were recorded by VF48 flash ADC manufactured by the TRIUMF national laboratory [10]. The VF48 had a 10 μs time range and was operated with a 25 MHz external clock signal.

3. Waveform analysis

3.1. Waveform model

The γ-ray energy and timing can be determined by fitting the CsI(Tl) output signal using a dedicated waveform model function. A typical waveform from the CsI(Tl) calorimeter is shown in the Fig. 3 (a), as indicated by black open circles. In the analysis, we adopted the following waveform formula,

$$f(t) = \frac{A}{1-\exp\{-(t-\tau_0)/\lambda)\}} \cdot Freq\left(\frac{t-\tau_0-d}{\mu}\right) \cdot \left\{\frac{t-\tau_0}{\tau_1}\exp\left(1-\frac{t-\tau_0}{\tau_1}\right) + \varepsilon\frac{t-\tau_0}{\tau_2}\exp\left(1-\frac{t-\tau_0}{\tau_2}\right)\right\}, \tag{2}$$

where A is the amplitude of the pulse and τ_0 is the rise time used for the timing determination. The λ, μ and τ_1, τ_2 parameters are time constants to express the rise and decay parts of the pulse, respectively. $d \sim 1$ μs is introduced for a timing adjustment and $\varepsilon \sim 0.06$ is the ratio of the two decay components. $Freq(x)$ is known as the frequency function given as

$$Freq(x) = \frac{1}{\sqrt{2}}\int_{\infty}^{x} exp(-t^2/2)dt. \tag{3}$$

Then, in order to determine these parameters, an equal-weighted χ^2 quantity is introduced,

$$\chi^2 = \sum_{i=1}^{250}\left\{A_i - f(t_i)\right\}^2, \tag{4}$$

where A_i and t_i are the ADC value and time of the ith waveform points, respectively. A_i is an integer number of the VF48 output and the bin by bin errors should be equal among all data points. The parameters in the model function were derived by minimizing the χ^2 values. The red line in Fig. 3 (a) is the fitting result using the above method, and the deviation of each data point (dh) is shown in Fig. 3 (b). Typical χ^2 values are distributed in the region of 100–500 (the number of degrees of freedom = 250 − 8 = 242) which is mainly due to the imperfect reproducibility of the CsI(Tl) output by the waveform model.

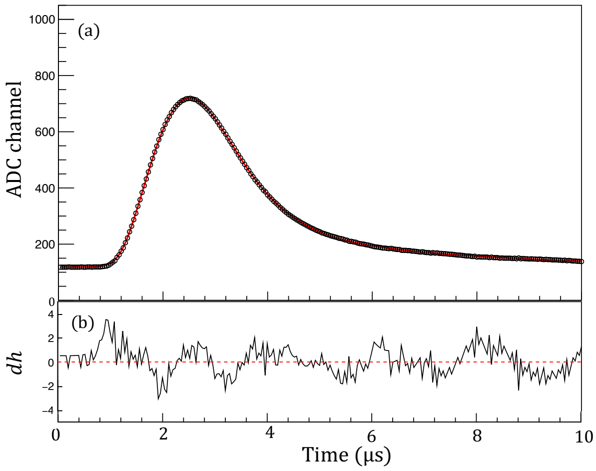

Fig. 3: (a) Typical waveform of the CsI(Tl) calorimeter signal. The open circles are the data and the red line is a fitting result of the waveform model. (b) The deviation of the data points from the fitting result.

3.2. Pulse separation of pileup events

For the analysis of pileup events, the maximum dh value ($dh_{\max}$) was first determined in the entire region using a single-pulse fitting. The waveforms with $|dh_{\max}| > 10$ can be recognized as two or more pulse components. The deviation of the data points from the single-pulse fitting result for a typical pileup event is shown in Fig. 4 (b), black line. These events were treated as pileup events, and multiple pulses in the fitting were taken into account. Then, the χ^2 value using a double-pulse waveform was again minimized by changing the fitting parameters. A typical pileup waveform is shown in Fig. 4 (a), black open circles. We can accept events as a double-pulse waveform with the conditions of (i) a waveform with $|dh_{\max}| < 10$ and (ii) the time interval between the 1st and the 2nd signals is greater than 200 ns. The rejected events are treated as events with further multiple signals. The red and green solid lines in Fig. 4 (a) are the fitting results using the single-pulse and double-pulse fitting functions, respectively. The associated decomposed pulses are shown as the green (1st pulse) and blue (2nd pulse) dotted lines. The thick red line in Fig. 4 (b) shows the dh distribution assuming the double-pulse fittings, which indicates successful pulse separation using the double-pulse fitting.

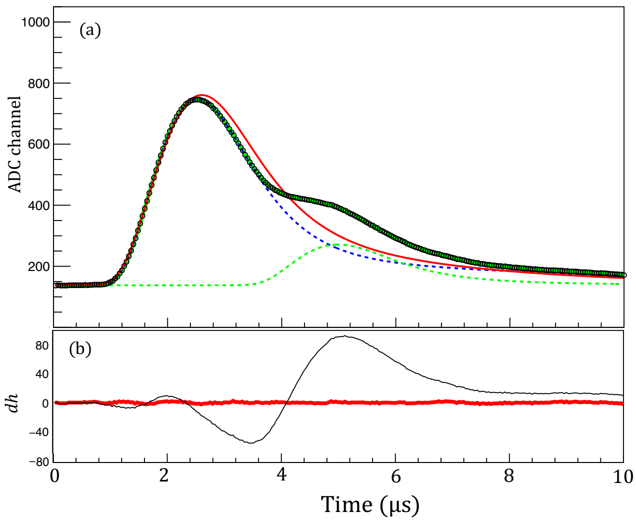

Fig. 4: (a) Typical pileup waveform of the CsI(Tl) calorimeter signal. The open circles are the data points. The red and green lines are the results adopting the single- and double-pulse fitting function. The green and blue dotted lines are the decomposed 1st and 2nd pulses. (b) The deviation of each data point from the fit curves. The black and red lines are the results using the single and double fitting, respectively.

4. CsI(Tl) calibration using $K_{\mu 2}$ decay events

4.1. *Background reduction by observing the e^+ from μ^+ decay*

The CsI(Tl) energy calibration was performed using mono-chromatic μ^+s from the $K_{\mu 2}$ decays at rest in the K^+ stopping target. The original μ^+ kinetic energy from stopped kaon decays was 152.5 MeV. These muons were stopped in the CsI(Tl) crystal after losing their energies in the target and generated the delayed e^+ signal from the subsequent $\mu^+ \to e^+ \bar{\nu_\mu} \nu_e$ decay. The e^+ signal can be observed as the second pulse in the waveform analysis using the double-pulse fitting.

The $K_{\mu 2}$ events were selected by the following conditions: (I) the number of hit crystals was only one, (II) the first pulse time coincided with the K^+ decay, and (III) the waveform data was successfully analyzed as a double-pulse waveform.

The pulse height spectrum obtained by selecting events with only the conditions (I) and (II) are shown in Fig. 5 as the black histogram. On the other hand, the red filled histogram represents events selected with all the above conditions. It is clearly seen that background components below the $K_{\mu 2}$ peak are significantly suppressed by requiring the μ^+ decay in the CsI(Tl). Here, the backgrounds are considered to be mainly accidental events created by the beam particles.

Then, the signal to noise ratio (S/N) was calculated as,

$$\mathrm{S/N} = \frac{N(500 \le l < 800)}{N(l < 500,\ 800 \le l)}, \tag{5}$$

where l is the pulse height of the first pulse obtained by the fitting. The $K_{\mu 2}$ peak region and the background dominant region were separated as $N(500 \le l < 800)$ and $N(l < 500,\ 800 \le l)$, respectively. The S/N ratio was determined to be ~ 0.4 for the events selected with the conditions of (I) and (II). Next, the μ^+ selection by requiring the double-pulse waveform was performed, and the S/N was obtained to be ~ 4. Thus, we can conclude that the requirement of the μ^+ stop and decay in the CsI(Tl) is a very useful technique to reduce the backgrounds from the beam particles and make the CsI(Tl) energy calibration significantly more accurate.

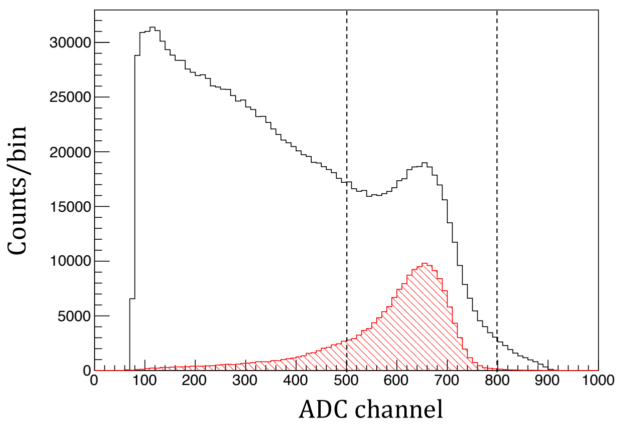

Fig. 5: Integrated pulse-height spectrum. The black spectrum shows the events selected with the conditions of (I) and (II). The red shaded histogram shows the events selected with all the conditions. The region indicated by the two dotted lines is used to estimate the S/N ratio.

4.2. *CsI(Tl) performance check*

For the CsI(Tl) energy calibration, the μ^+ energy loss in the target system should be added to the μ^+ energy observed by the CsI(Tl). The energy conversion factor, k, can be formulated as $k = (152.5 - E_t \text{ MeV})/l$, where E_t is the muon energy loss in the target. The μ^+ path length in the target was obtained by connecting the CsI(Tl) center of the μ^+ hit module and the K^+ vertex position determined by the target system. The typical k value was obtained to be 2.1–2.5 MeV^{-1}. Then, the μ^+ energy spectrum from the $K_{\mu 2}$ decay is obtained by taking into account the energy loss in the target as $E = kl + E_t$, as shown in Fig. 6. The red and blue spectra indicate the calibrated energy spectrum with and without the target energy correction, respectively. The target energy correction improved the energy resolution to σ=2.63% from 4.73%.

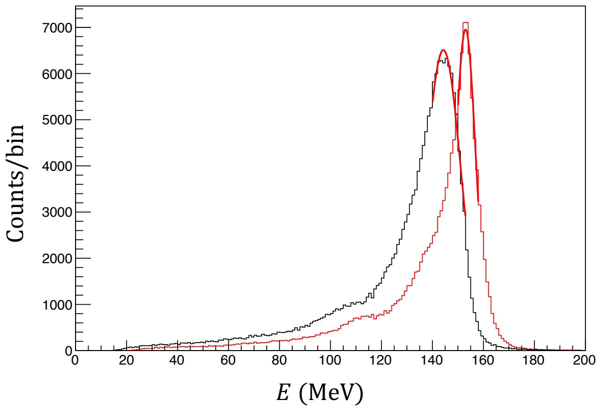

Fig. 6: The calibrated energy spectra obtained using the $K^+ \to \mu^+ \nu_\mu$ decays. The red spectrum includes a correction for the energy loss in the target. The red lines are the fitting results assuming a Gaussian function.

Also, the CsI(Tl) timing information was checked by requiring the e^+ signals to reduce the effects from accidental backgrounds. The 40 ns clock timing uncertainty of VF48 was corrected for by measuring the trigger signal timing using the same VF48 module ($T_{\rm ref}$). Fig. 7 shows the μ^+ timing distribution obtained from the τ_0 parameter corrected for $T_{\rm ref}$, $\tau_0 - T_{\rm ref}$. The timing resolution was determined to be $\sigma = 10.7 \pm 0.1$ ns by fitting the distribution with a Gaussian function, as shown by the red line in Fig. 7.

5. A new method of energy calibration using stopped comic-ray muons

It is possible to consider a new CsI(Tl) calibration method using stopped cosmic-ray muons with the subsequent e^+ emission in the CsI(Tl) calorimeter [11]. This method is proposed to measure the e^+ energy spectrum for a rough CsI(Tl) energy calibration without using the $K_{\mu 2}$ decays. Since the maximum e^+ energy from the muon decay is 52.32 MeV,

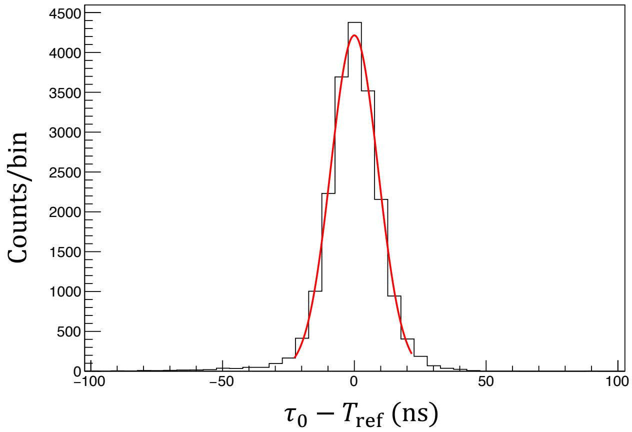

Fig. 7: The μ^+ timing distribution corrected for $T_{\rm ref}$ ($\tau_0 - T_{\rm ref}$). The timing resolution was determined to be $\sigma = 10.7 \pm 0.1$ ns.

the energy calibration can be performed by measuring the e^+ energy after the cosmic-ray muon stops in the CsI(Tl) crystal. The cosmic muons stop homogeneously in the CsI(Tl), and we do not need to consider the specific structure of the CsI(Tl) calorimeter.

The energy distribution of the decomposed second pulse is shown in Fig. 8 as indicated by the black dots. Here the calibration parameters obtained from the $K_{\mu 2}$ decays were used. The red squares and black open circles are the calculated e^+ and e^- energy distributions from stopped cosmic μ^+ and μ^- decays, respectively, obtained using a Monte Carlo simulation based on a GEANT4 code. Electromagnetic shower leakage from the muon stopped module was taken into account. The energy distributions were calculated by varying the muon yield ratio of F_+/F_- =1.1–1.6 [12–16] and compared with the experimental one. The green line shown in Fig. 8 is the result with $F_+/F_- = 1.6$. The energy resolution of 2.63% in σ obtained from the $K_{\mu 2}$ calibration result has been used.

In order to determinate the energy calibration parameters using stopped cosmic-ray muons, a common gain parameter relative to the energy coefficients obtained from the $K_{\mu 2}$ calibration results was introduced. The reduced χ^2_ν/NDF determined by comparing the experimental data with the simulation was calculated as a function of the above relative gain coefficient, as shown in Fig. 9, where NDF is the number of degrees of freedom. The black dots and open squares correspond to the results obtained by assuming $F_+/F_- = 1.1$ and 1.6,

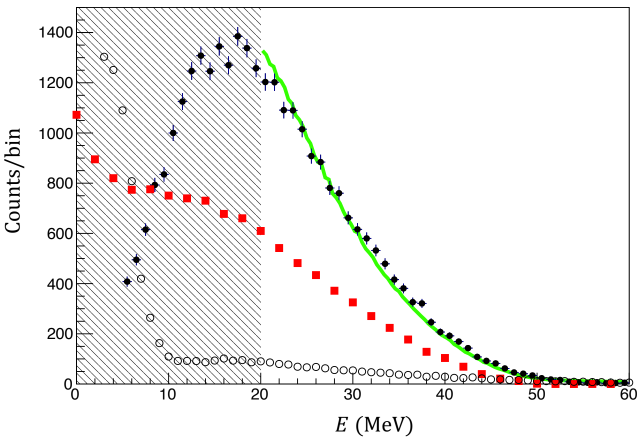

Fig. 8: Energy distributions of e^+ (e^-) from stopped cosmic muons. The red squares and black open circles are the calculated e^+ and e^- energy distributions, respectively. An electromagnetic gamma shower was taken into account in the simulation. The black hatched area is not used in the fitting because of the online threshold setting of 20 MeV.

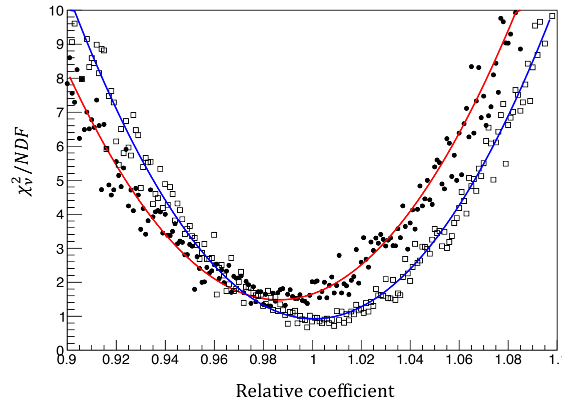

Fig. 9: Reduced χ^2_ν obtained by changing the relative gain coefficient. The black dots and open squares correspond to the results obtained by assuming $F_+/F_- = 1.1$ and 1.6, respectively. The lines in the figure represent the fitting results using a parabolic function. The gain coefficients obtained from the stopped cosmic muons are consistent with those from the $K_{\mu 2}$ events within 3–4%.

respectively. It should be noted that the fitting region was chosen to be 20–60 MeV because the online energy threshold was set to 20 MeV. Scattering of the χ^2_ν values is due to random smearing to account for the CsI(Tl) energy resolution. The lines in the figure represent the fitting results using a parabolic function. As a result, the relative coefficients for $F_+/F_- = 1.1$ and 1.6 were determined to be 0.986 ± 0.033 and 1.001 ± 0.032, which indicates the gain coefficients obtained from the stopped cosmic muons are consistent with those from the $K_{\mu 2}$ events at the 3–4% level. Therefore, the experimental data were in good agreement with the above two simulation models, indicating a correct understanding of the e^+ and e^- behavior generated from the stopped muons.

The muon lifetime curve was also measured using the time interval between the 1st and 2nd pulses, as shown in Fig. 10 by the black dots. The pulse separation efficiency of events with the first and second pulse time difference shorter than 1 μs is very low. The fall off of the data points higher than 8 μs is due to the finite 10 μs window of the VF48. Fitting the data with an exponential function, the decay constant was determined to be 2.06 ± 0.03 μs ($\chi^2_\nu/NDF = 69.5/43$), as shown by the red line. The fitting region of 3.5–8.0 μs was chosen, since the second pulse separation efficiency was not significantly high out of this region. The observed time constant is a little shorter than the PDG value which indicates that most of the μ^- events are captured by CsI nuclei and do not contribute to the above lifetime measurement.

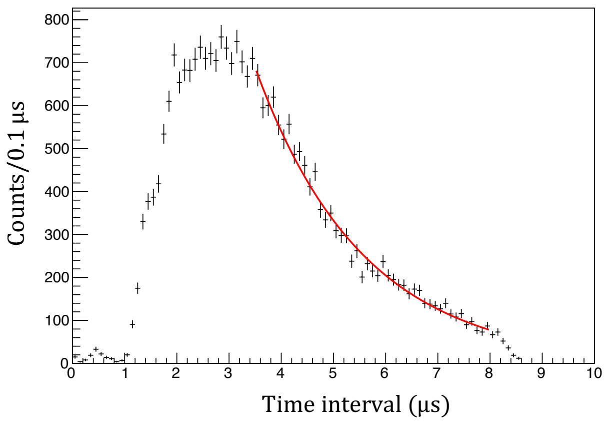

Fig. 10: Time interval between cosmic muons and the delayed e^+ (e^-) signals through the $\mu \to e\nu\bar{\nu}$ decays. The black dots and the red line are the data and fitting function, respectively.

6. Conclusion

A model function for the waveform analysis of the CsI(Tl) calorimeter in the E36 experiment has been developed, and the information of the decomposed second pulses can be used for the event selection. The CsI(Tl) energy calibration was successfully performed by choosing the $K_{\mu 2}$ events, and imposing the existence of the second pulses, and the S/N ratio was significantly improved. Then, the CsI(Tl) performance was carefully checked by studying the energy and timing resolutions.

A new energy calibration method using stopped cosmic muons is proposed. The energy and timing of the delayed e^+ (e^-) signals were determined by the decomposed second pulse in the double-pulse waveform analysis. The observed energy spectrum is consistent with the simulation calculation with an accuracy of 3–4%, indicating the establishment of a new calibration method without using any accelerator facilities.

Acknowledgement

This work was supported by a Grant-in-Aid for Scientific Research (C), No. 15K05113, from the Japan Society for the Promotion of Science (JSPS) in Japan and by NSERC and NRC (TRIUMF) in Canada. The authors thank H. Yamazaki for encouragement in executing this work. We would like to thank the J-PARC staff for the excellent beam delivery during our experimental beamtime.

References

[1] G. Lamanna et al., Nucl. Part. Phys. Proc. **273-275** (2016) 1671.
[2] C.Lazzeroni et al., Phys. Lett. B **719** (2013) 326.
[3] F. Ambrosino et al., Europ. Phys. J. C **64** (2009) 627.
[4] V. Cirigliano and I. Rosell, Phys. Rev. Lett. **99**, 231801 (2007).
[5] S. Shimizu, et al., Proposal for J-PARC 50 GeV Proton Synchrotron, P36 Jun 2010.
[6] S. Strauch et al., Proc. Scie., PoS(KAON13)014, 2013.
[7] M. Abe et al., Phys. Rev. D **73,** 072005 (2006).
[8] J.A.Macdonald et al., Nucl. Instrum. Methods A **506** (2003) 60.
[9] D.V. Dementyev et al., Nucl. Instrum. Methods A **440** (2000) 151.
[10] Y. Igarashi and M. Saito, in: IEEE 2012 Nuclear Science Symposium and Medical Imaging Conference Record (NSS/MIC), DOI: 10.1109/NSS-MIC.2012.6551335.
[11] H. Ito et al., in: IEEE 2016 Nuclear Science Symposium and Medical Imaging Conference Record (NSS/MIC), DOI: 10.1109/NSSMIC.2016.8069751.
[12] S. Haino et al., Phys. Lett. B **594**, 35 (2004).
[13] P. Archard et al., Phys. Lett. B **598**, 15 (2004).
[14] P. Adamson et al., Phys. Rev. D **76**, 052003 (2007).
[15] V. Khachatryan et al., Phys. Lett. B **692**, 83 (2010).
[16] N. Agafonova et al., Eur. Phys. J. C **67**, 25 (2010).

Figure1

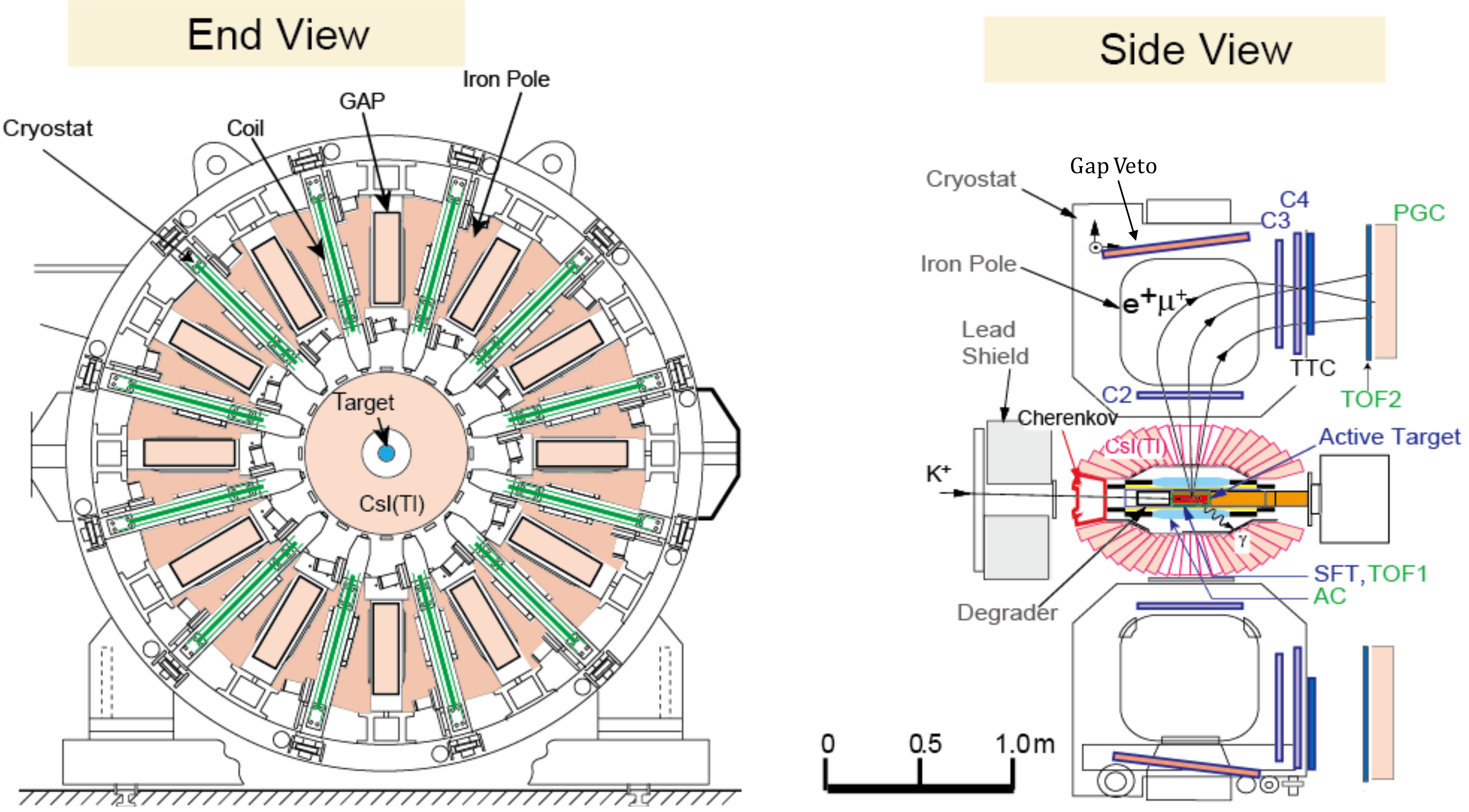
End View
Iron Pole
GAP
Cryostat
Coil
Target
CsI(Tl)
Side View
Gap Veto
Cryostat
C4
C3
PGC
Iron Pole
Lead
Shield
TTC
C2
TOF2
Cherenkov
Active Target
CsI(Tl)
K+
γ
SFT, TOF1
AC
Degrader
0
0.5
1.0m

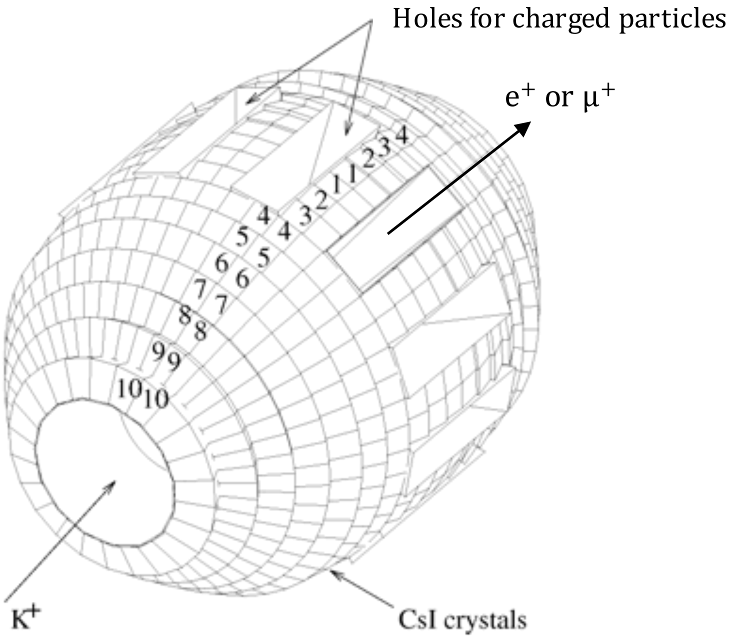
Holes for charged particles
e+ or μ+
K+
CsI crystals
1 2 3 4
1 2 3 4
4 5 6 7 8 9 10
5 6 7 8 9 10

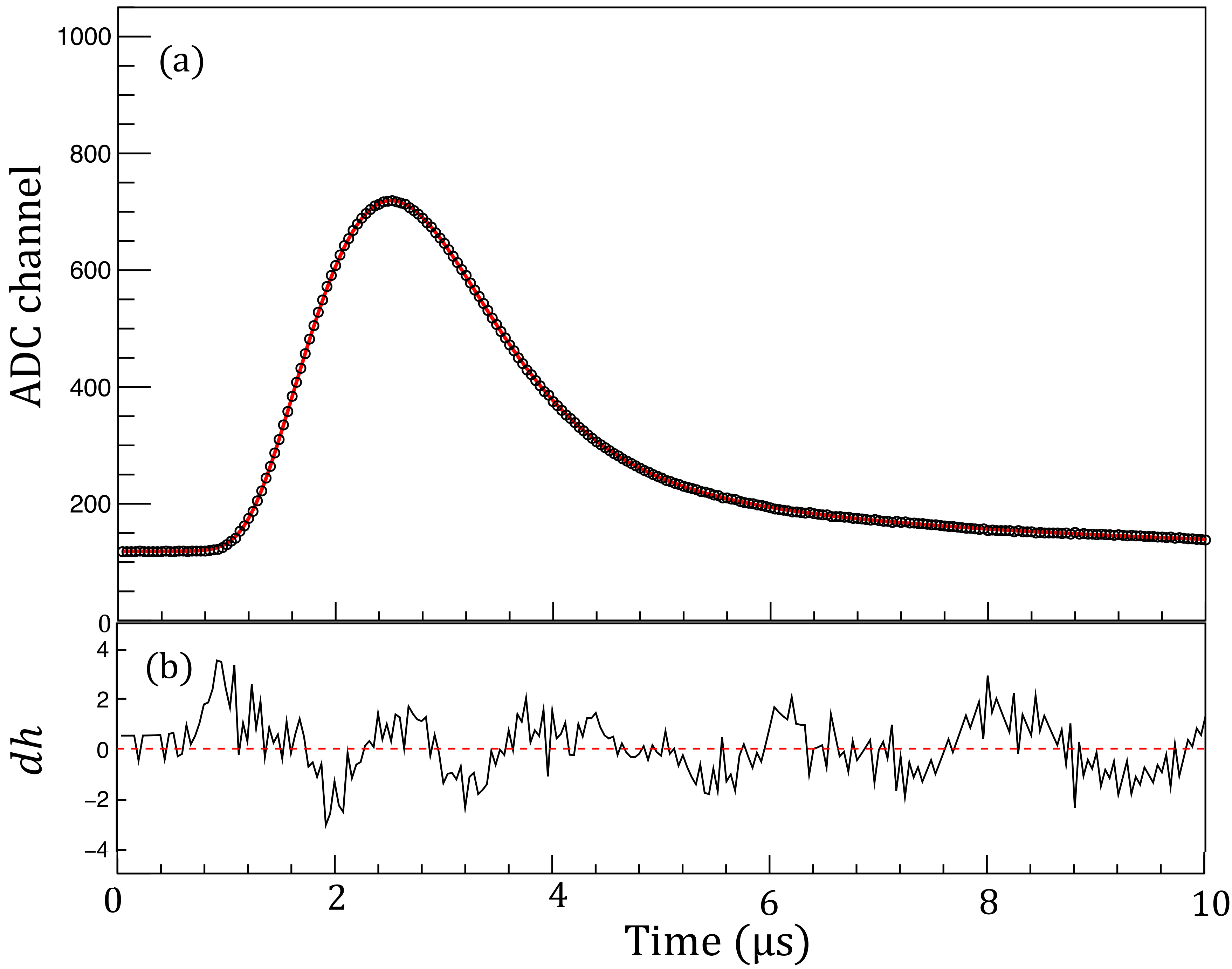

(a)
(b)
ADC channel
dh
Time (μs)
0
200
400
600
800
1000
4
2
0
−2
−4
0
2
4
6
8
10

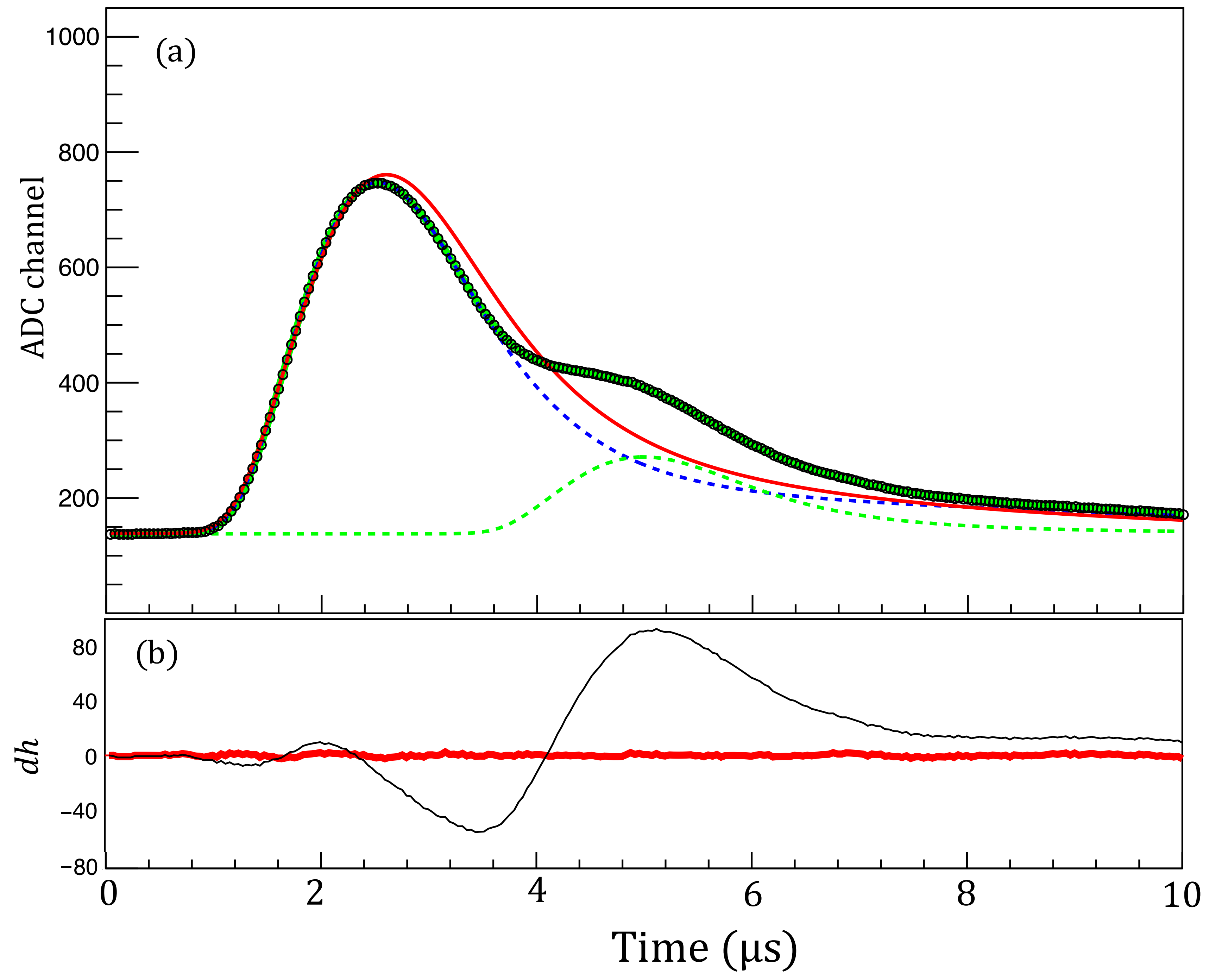
(a)
ADC channel
1000
800
600
400
200
(b)
dh
80
40
0
−40
−80
0
2
4
6
8
10
Time (μs)

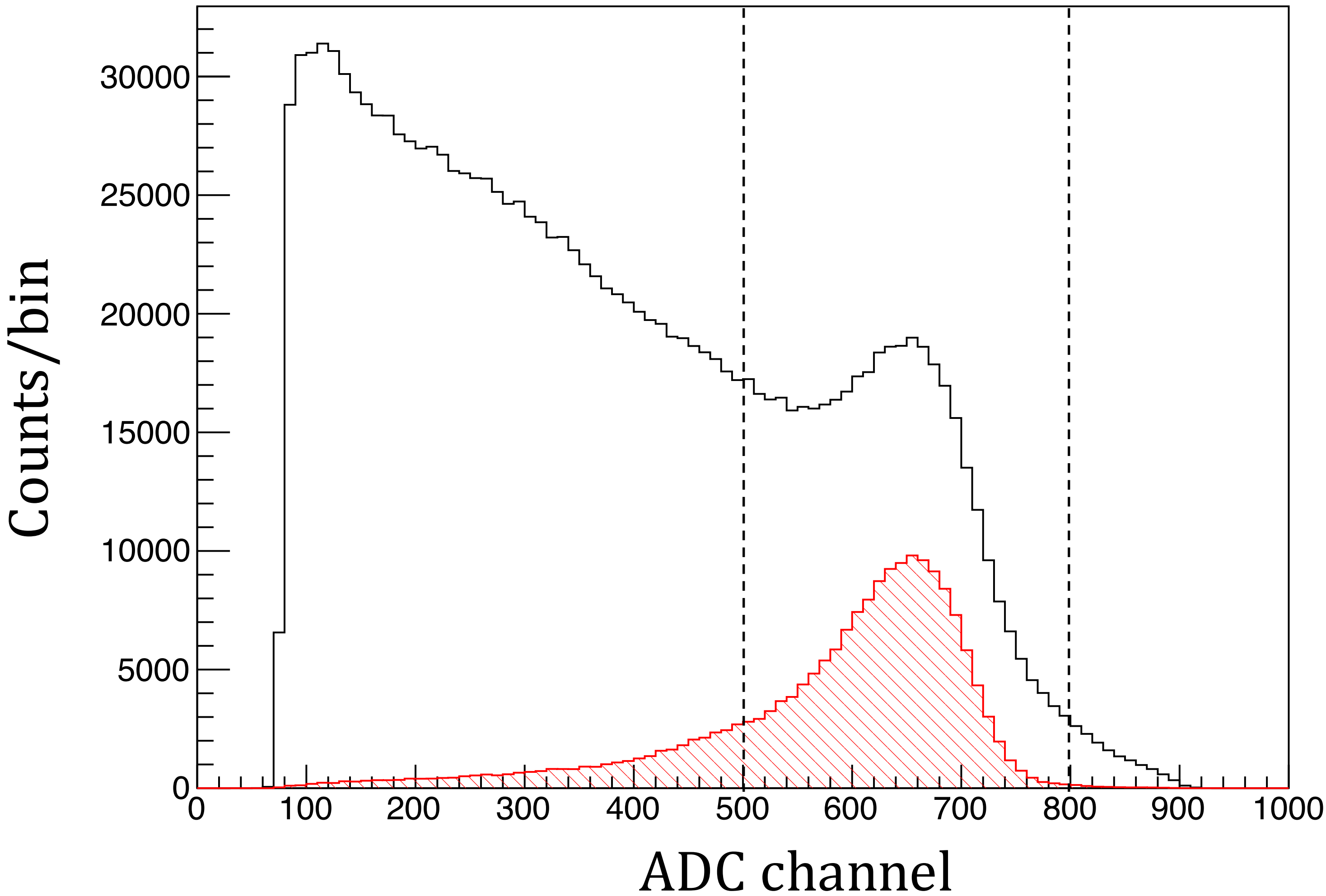
Counts/bin
30000
25000
20000
15000
10000
5000
0
0
100
200
300
400
500
600
700
800
900
1000
ADC channel

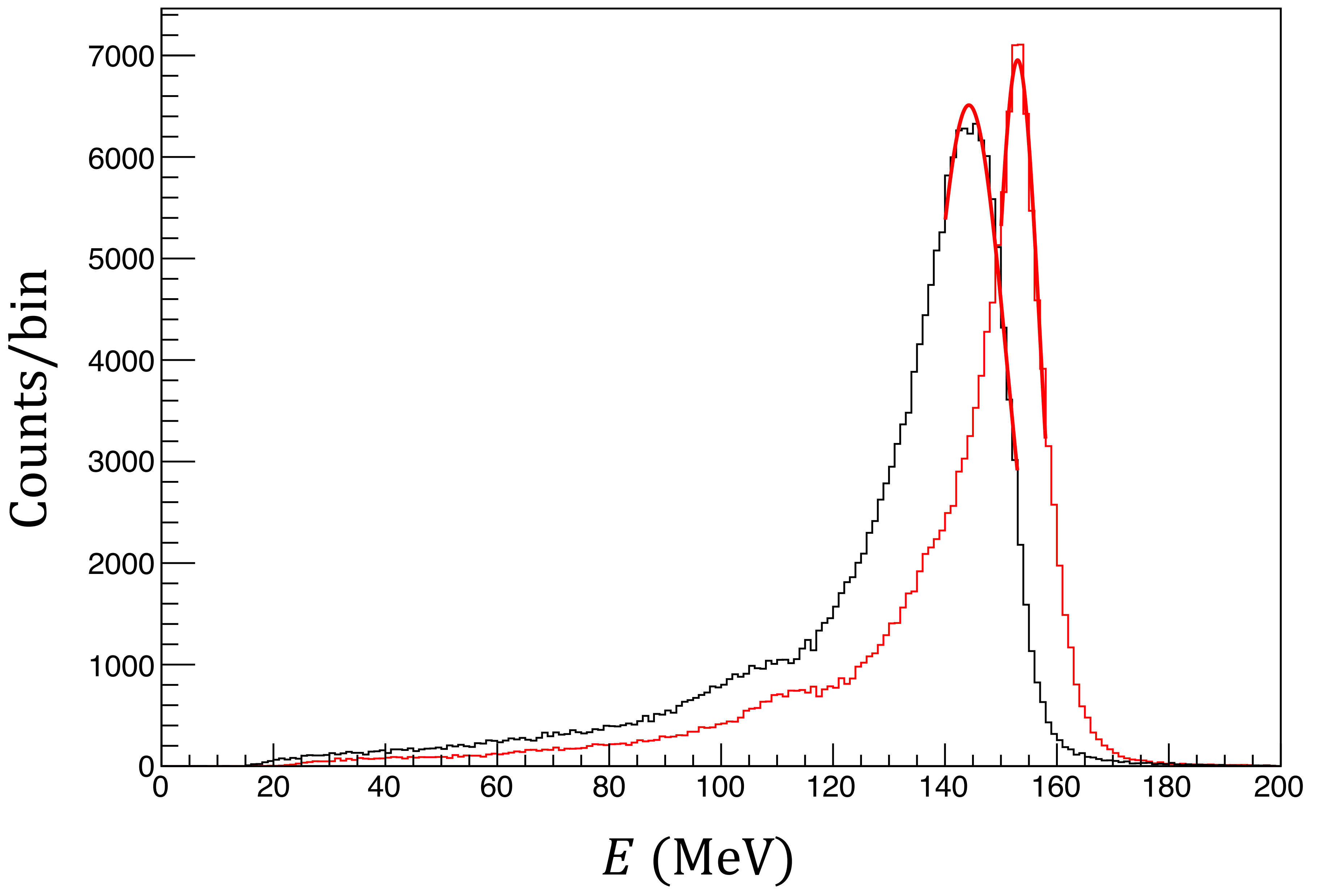

Counts/bin
0
1000
2000
3000
4000
5000
6000
7000
0
20
40
60
80
100
120
140
160
180
200
E (MeV)

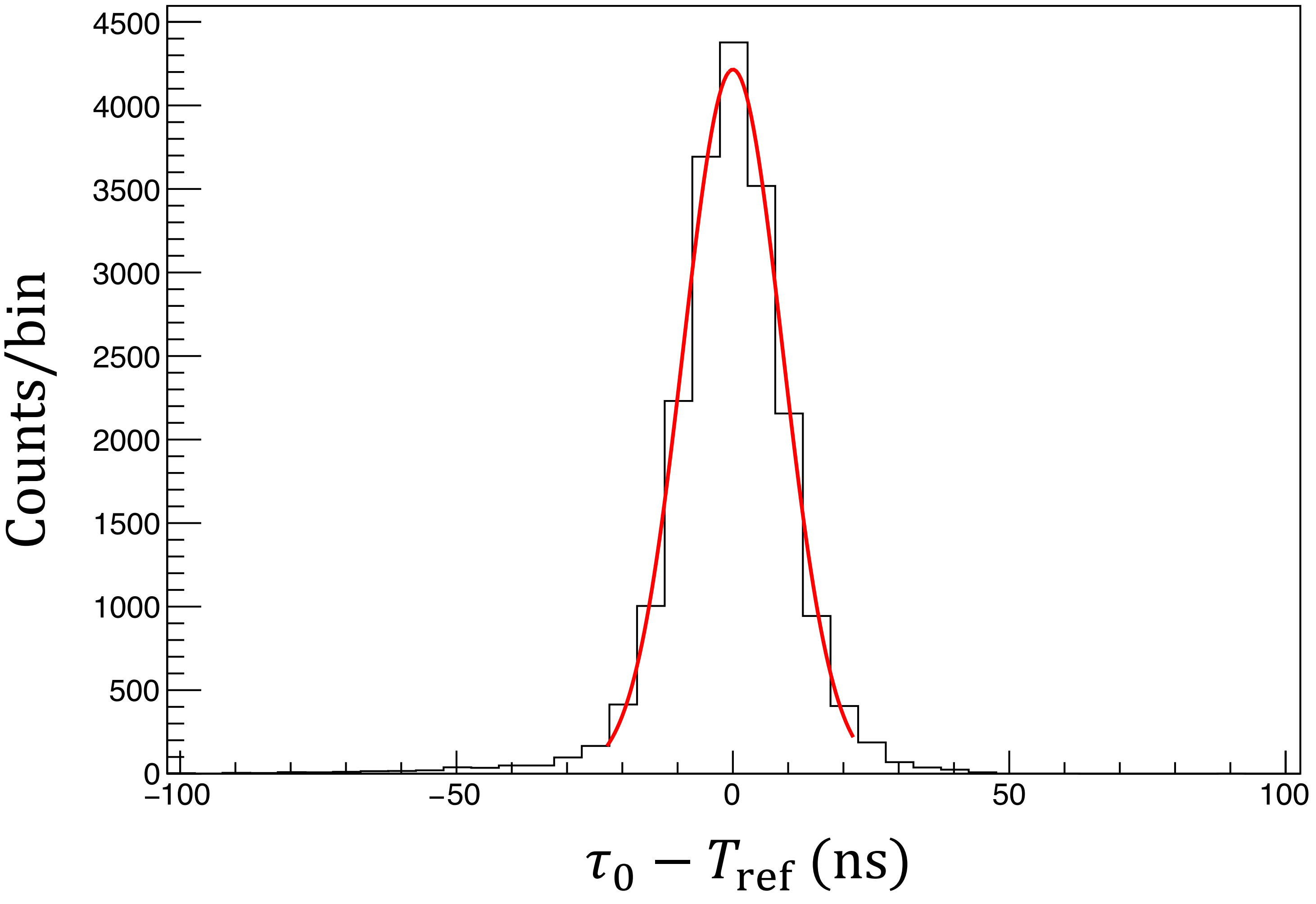

Counts/bin
4500
4000
3500
3000
2500
2000
1500
1000
500
0
−100
−50
0
50
100
$\tau_0 - T_{\mathrm{ref}}$ (ns)

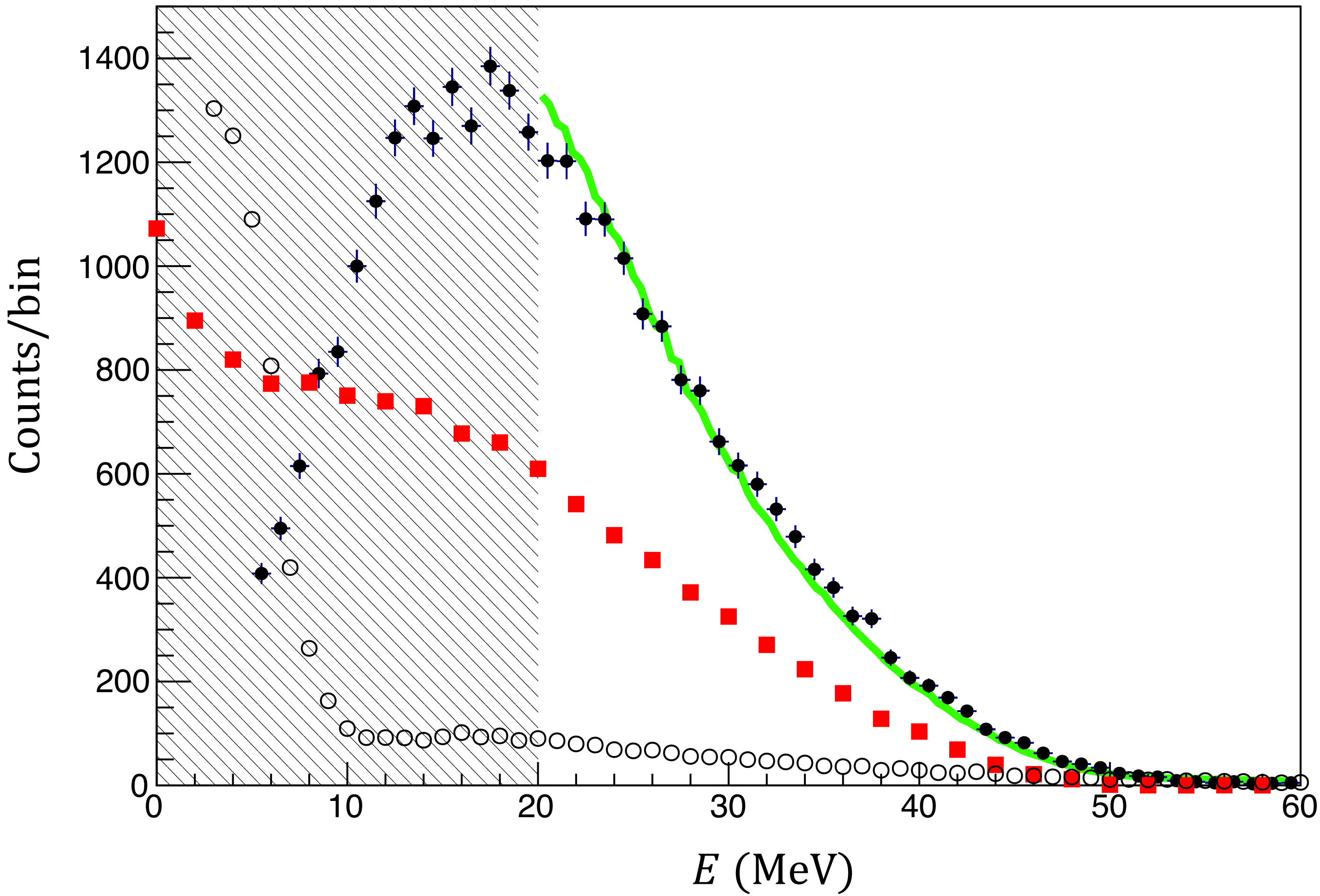

Counts/bin
0
200
400
600
800
1000
1200
1400
0
10
20
30
40
50
60
E (MeV)

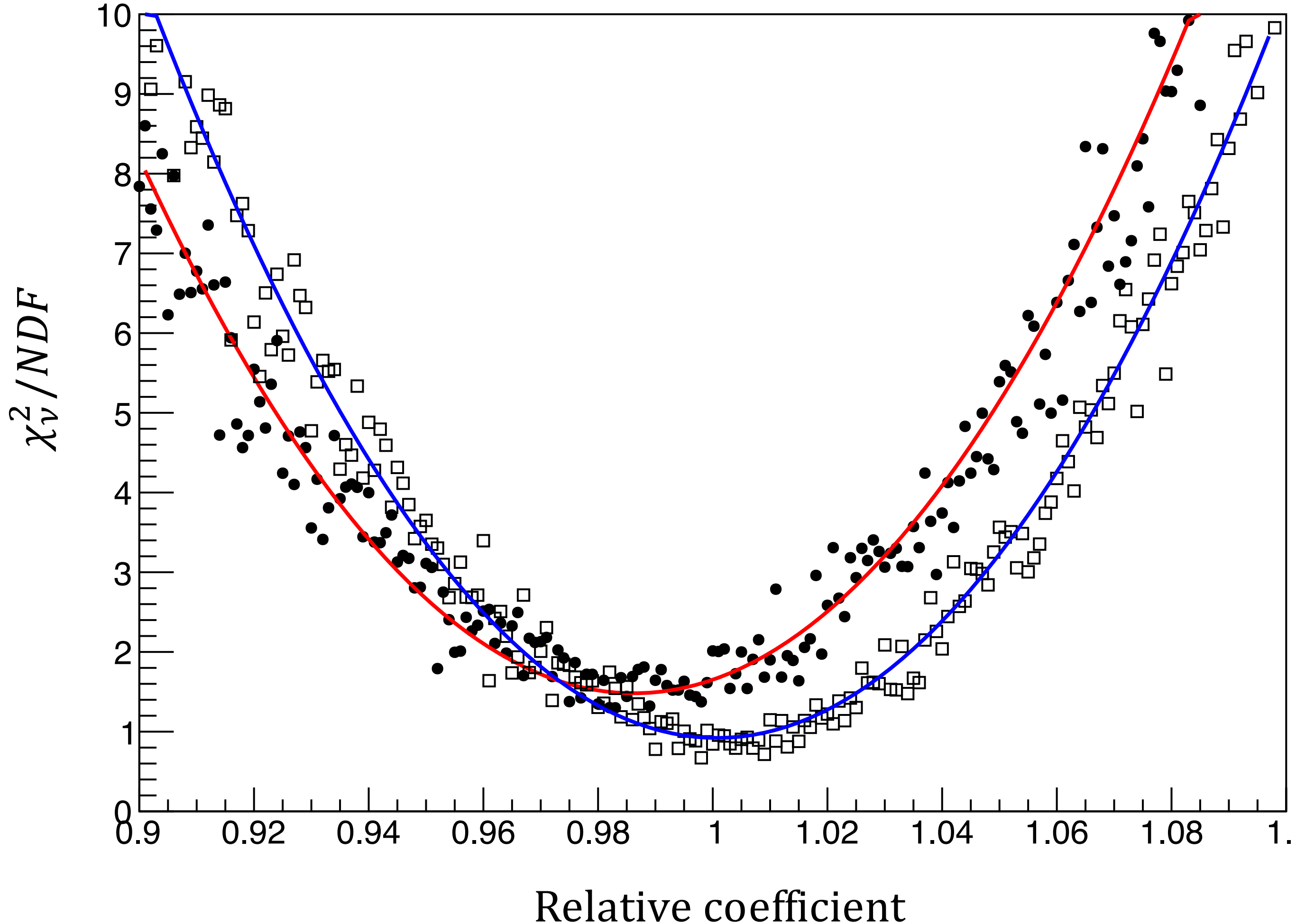

χ_v^2/NDF
Relative coefficient
0
1
2
3
4
5
6
7
8
9
10
0.9
0.92
0.94
0.96
0.98
1
1.02
1.04
1.06
1.08
1.1

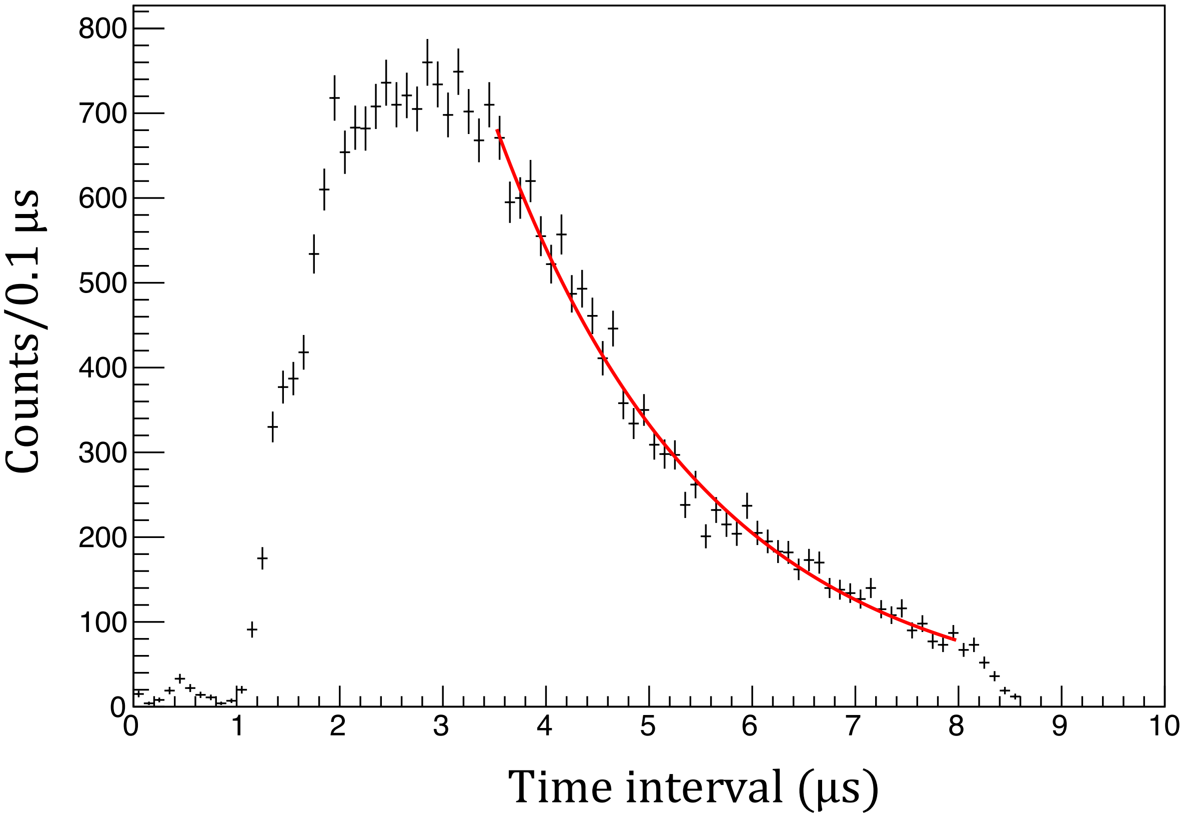

Counts/0.1 μs
800
700
600
500
400
300
200
100
0
0
1
2
3
4
5
6
7
8
9
10
Time interval (μs)

*Response to Reviewers &/or Editor

Reviewer #1:
Referee report on the Manuscript NIMA-D-18-00091

Introduction

The article describes an interesting calibration technique of the CSI(Tl) crystals for the J-PARC E36 experiment based on muons from kaon decays, and cosmic ray stopped muons.
The double peak search technique, based on the analysis of signal time structure, is rather new and produce significant improvements in the E36 calorimeter calibration.
The results obtained are interesting enough so that the paper deserves publication.

General comments
The figures are in general difficult to read in black and white printing. In particular in Fig. 3b it's very difficult to see the red line. I suggest to use thicker lines and use different type of dashed lines.
The figure is updated and we changed the text in line 124 "thick red line in Fig. 4(b)" from "red line in Fig. 3(b)". Figure number was changed because we added a new figure (explained below).
In Fig.2 Fig.3 the x axis is labelled as "TDC channel". I think this is misleading if you are using a FADC as described in the text. I'll suggest to convert the x axis in (ns). In this way it will be easier to understand the text where all the reference are in units of seconds.
The figure is updated.
Figure 6. Difficult to distinguish blue squares from red open circle.
The figure is updated to Fig.8 and we modified the text in line 227 "The energy distributions were calculated by varying the muon ratio F+/F-=1.1-1.6 and compared with the experimental one. The green line shown in Fig.8 is the result with F+/F-=1.6".

Minor comments
- Line 21: make -> perform.
We changed the text following this suggestion.

- Line 54: The size of the crystal expressed in angular coverage (7.5$^¥circ$) is difficult to understand. I suggest to use the crystal size in cm.

The crystal shape is trapezoidal, depending on their position. It is difficult to express the crystal size in cm unit. We added a new figure (Fig.2) to help the understanding the calorimeter structure.

- Line 55-56: "The length of the CsI(Tl) crystal was 25 cm which was enough to obtain sufficient energy resolution as well as avoid nuclear counter effects."

The sentence is too vague. What is the required energy resolution? What are the "nuclear counter effects" you want to avoid?

We modified the text of line 57-58 as "which was long enough to neglect shower leakage from the rear end".

- Line 93: Will be useful to add the NDOF to judge the value of the <chi>^{2}

The discussion of the chi^2 value is not simple because the error of each dot can be separated into (1)electric noise and (2)systematic effect from imperfect reproducibility of the waveform function. Here, the NDOF=250-8=242 and the chi^2 value is distributed 100-500. Therefore the error size is considered to be fluctuating event-by-event in the region 0.6-1.4. We added the text in line 97 "the number of degree of freedom is 250-8=242."

- Line 100: the sentence needs an improved English

We changed the text of line 105 from "two or more than two pulse components" to "two or more pulse components"

- Line 130: "152.5 MeV". It would be better to specify why the energy of the muons is so exactly defined

We modified the text of line 134 from to "The original ¥mu+ kinetic energy from stopped K+ decays"

and we modified the text of line 136 from "in the CsI(Tl) crystal and …" to "in the CsI(Tl) crystal after losing their energy in the target and …".

- Line 144: "the red histogram represents events" -> the red filled histogram represents events

We changed the text following this suggestion.

- Line 147: "significantly removed" -> significantly suppressed
We changed the text following this suggestion.
- Line 158: "selected with the conditions of (1)(2)." -> selected with the conditions of (I)(II)
We changed the text following this suggestion.
- Line 191: too few information on the time resolution. A figure and a short comment will help judging.
We changed the text in line 78-79 "and tau0 is the rise time used for the timing determination" and the text in line 197 "Fig.7 shows the ¥mu+ timing distribution obtained from the tau0 parameter corrected for Tref, tau0-Tref, and a new figure (Fig.7) for the CsI(Tl) timing spectrum was added.
- Line 199: "radioactive beam." I don't like the definition radioactive beam if it refers to muons from K_{m2} decays
We modified the text of line 210 from "without using radioactive beam" to "without using the Kmu2 decays".
- Line 212: Please be more specific on the source of the e^+ e^- namely μ^+ $\mu-$ decay.
We modified the text of line 222 from "the calculated e+ e- energy distributions, respectively" to "the calculated e+ e- energy distributions from stopped cosmic mu+ and mu- decays, respectively".
- Paragraph starting at line 249. Why the fitting starts at 3.5μs? I guess before that time difference the two pulse cannot be distinguished well enough? please comment.
Yes, the two pulses cannot be decomposed well, and the efficiency of the second pulse separation depends on the time difference of the two pulses and the height of the second pulse. In this sense, the life time spectrum before 3.5 micro sec was deformed and cannot be used for the life time measurement. We added the text of "The fitting region of 3.5-8.0 micro sec was chosen, since the second pulse separation efficiency was not significantly high out of this region." at line 271.

========================

Reviewer #2:

The article treats the performance of the CsI calorimeter of J-Parc experiment E36.

The article is well written and should be published, I would however request a couple of clarifications:

- section 2: Eq 4 and Fig2a and b: an equal weight chi**2 is used and the waveform functions fits the rising edge, falling edge as well as the pedestal. On the example waveform the pedestal part (up to channel 40) has a pull between +2 and -4 and one of the requirement of the multiple pulse detection is 10.

    - is this a "typical" pull?

    Yes, this is a typical pull. Unfortunately, we could not pick up the same pulse figure shown in Fig.3 in the last version, because we just chose one of typical figures. Now Fig.3 was replaced by another typical pulse.

    - are the bin by bin errors equal? (if yes, it would be good to state that because it makes the choice of the chi**2 easier to understand.

    We added the text in line 89 "Ai is an integer number of the VF48 output and the bin by bin errors should be equal among all data points."

    - how strongly does the baseline/pedestal part of the signal influence the fit results?

    The baseline fluctuation was obtained to be sigma=1.23ch which corresponds to 0.2% of the Kmu2 peak of 152.5 MeV. Therefore, the baseline part does not strongly influence the energy resolution.

- the tau_i (i=0,1,2) parameters are determined in each fit? Are their distributions (ie average value) as expected?

Yes, the tau values were the fitting parameters in each time, which were obtained tau0~1, tau1~0.7, and tau2~1.7 (micro sec) in each fit

- the chi**2 of 100 as fit result sounds large, but shouldn't this be put in perspective by dividing by the error**2 and the degrees of freedom of the fit?

The discussion of the chi^2 value is not simple because the error of each dot can be separated into (1)electric noise and (2)systematic effect from imperfect reproducibility of the waveform function. Here, the

NDOF=250-8=242 and the chi^2 value is distributed 100-500. Therefore the error size is considered to be fluctuating event-by-event in the region 0.6-1.4. We added the text in line 97 "the number of degree of freedom is 250-8=242."

Section 4:

Eq 5: how were the lower and upper bounds chosen to define the sidebands?

There are no strong scientific reasons. The uncertainty of the S/N ratio is not very important and we changed 0.42→0.4 and 4.42→4 at line 164 and 167.

On the other hand, the pi+s from K+→pi+ pi0 also contribute to this spectrum around 500ch. We wanted to remove these pi+ events.

Figure 4: since the figure is integrated over modules and in units of ADC, wouldn't it make sense to be quantitative about the uniformity of the electronics? Wouldn't a large electronics dispersion also contribute to the width?

The width of Fig.4 is mainly due to (1) electronics dispersion (gain fluctuation) of the modules and (2) uncorrected energy loss in the target. Their contributions to the width are comparable.

Figure 8:

- is the fall off of the data points at large times (not included in the fit) due to the finite 10us window? If yes, it would be good to mention that.

We added the text in line 266 "The fall off of the data points higher than 8us is due to the finite 10us window of the VF48."

- the position of the rising edge should be explained (minimum deltaT for the pulses seems to be 1us, where 200ns were mentioned in the previous chapter

In the fitting code, we required 200 ns for the minimum time difference. However, the separation efficiency shorter than 1us is very low. Therefore, we added the text in line 263 "The pulse separation efficiency of events with the first and second pulse time difference shorter than 1 us is very low"

- the explanation of the reduced muon lifetime is not clear: why does the capture deform the signal instead of reducing with equal probability the counting rate independent of time?

The muon decay and muon capture is competitive processes and it is known the effective mu- life time in materials becomes short depending on Z number of stopper materials.

- is the 10us TDC time window triggered by the muon? If not, a random offset in the time window can also bias the distribution towards lower lifetimes. Please clarify.

We also measured the muon incident time using the same VF48 FADC and corrected the timing for it event-by-event. In this sense time window was triggered by the muon. A new figure for the CsI(Tl) timing spectrum was added. We changed the text in line 78-79 "and tau0 is the rise time used for the timing determination" and the text in line 197 "Fig.7 shows the ¥mu+ timing distribution obtained from the tau0 parameter corrected for Tref, tau0-Tref, and a new figure (Fig.7) for the CsI(Tl) timing spectrum was added. We changed the text in line 199 "The timing resolution was determined to be sigma = 10.7 +/- 0.1 ns by fitting the distribution with a Gaussian function, as shown by the red line in Fig.7."

==============================

Reviewer #3:

Comments to the authors

Please find in the following a list of comments for your consideration.

Abstract - line 1, replace "for a lepton universality" with " for lepton universality"

We changed the text following this suggestion.

23 - I would add that the data taking was completed in 2015. In this way the sequence of tenses is more understandable

We added the text in line 23 "The experiment was performed in 2015."

28 - fig 1 would be better placed at the top of pag. 2, if possible

We changed the text following this suggestion.

51 - it is not specified where the 12 holes are placed; please rephrase

The crystal shape is trapezoidal, depending on their position. It is difficult to express the crystal size in cm unit. We added a new figure to help the understanding the calorimeter structure.

77 - line 5, remove article "the"

We changed the text following this suggestion.

77 - line 8, remove "as"

We changed the text following this suggestion.

86 - remove "as"

We changed the text following this suggestion.

90 and 109 - data points drawn as open black circle in fig. 2 and 3 are not clearly visible

The figures are updated.

103 - replace "Fig. 3 (b) as the black line" with " Fig. 3 (b), black continuous line"

We changed the text following this suggestion.

109 - replace "Fig. 3 (a) as the black open circles" with " Fig. 3 (a), black open circles"

We changed the text following this suggestion.

112 - replace "<10, (ii) the" with "<10 and (ii) the"

We changed the text following this suggestion.

113 - replace "longer" with "greater"

We changed the text following this suggestion.

130 - how is determined the kinetic energy of the stopped muons? Add just a short sentence

We modified the text of line 134 from "The mu+ kinetic energy was 152.5 MeV" to "The original muon kinetic energy from stopped K+ decays was 152.5 MeV"

and we modified the text of line 136 from "in the CsI(Tl) crystal and …" to "in the CsI(Tl) crystal after losing their energy in the target and …".

142 - replace "the conditions of only (I) (II)" with "only the conditions (I) and (II)"

We changed the text following this suggestion

Fig. 4 - Use the same symbols in Fig 4 (numbers 1 and 2) as in the text

We changed the text following this suggestion

158 - same as above, use consistent numbering for selection conditions: I II III or 1 2 3 all along the text.

We changed the text following this suggestion

159 - add a comma after Next

We changed the text following this suggestion.

171 - the conversion factor k is per unit length? In other words, "l" is the path?

The l parameter is the pulse height and k is a conversion factor of MeV/ch.

185 - it is not clear how the timing resolution is determined i.e. how the e+ signals reduce the accidental background

We changed the text in line 78-79 "and tau0 is the rise time used for the timing determination" and added the text in line 197 "Fig.7 shows the mu+ timing distribution obtained from the tau0 parameter corrected for Tref, tau0-Tref. The timing resolution was determined to be sigma = 10.7 +/- 0.1 ns by fitting the distribution with a Gaussian function, as shown by the red line in Fig.7."

and a new figure for the CsI(Tl) timing spectrum was added.

212 - replace "distribution" with "distributions"

We changed the text following this suggestion.

212 and Fig. 6 caption - indicate the colours for e+ and e- also in the caption

We added the text in caption of Fig.8 “The red squares and black open circles are the calculated e+ and e- energy distributions, respectively.”

216 - Fig 6 is ok, but the red cross-hatched and the green filled regions almost overlap and it is hard to distinguish differences without zooming

The figure is updated. The energy distribution obtained assuming the muon ratio F+/F-=1.6 is only shown in the figure.

227 - remove one "the"

We changed the text following this suggestion.

234 - "The black hatched area…." either add "in fig. 6" or remove completely the sentence (already stated one line above).

We remove the sentence.

256 - "theoretical value"? In general the measured values are compared to the PDG value

We changed the text following this suggestion.

261 - replace "of CsI(Tl) calorimeter" with "of the CsI(Tl) calorimeter"

We changed the text following this suggestion.

265 - replace "events and imposing" with " events and, imposing"

We changed the text following this suggestion.

I recommend to add to the reference list the paper "Development of a versatile calibration method for electromagnetic calorimeters using a stopped cosmic-ray beam", published in IEEE Xplore, DOI: 10.1109/NSSMIC.2016.8069751 , in which the method is also described.

We added the reference.